in a nine-coordinate solvated dimeric form (Table I).

Too little data are available to generalize further. However, as more structural information is gathered and the quantitative analysis of steric factors in organolanthanide chemistry becomes more refined,[53,54] it may be possible to predict which ligand-metal combinations will be flexible and which will not. This could be quite useful in controlling reactivity.[2]

Another conclusion obtainable from this study is the importance of the steric bulk of $(C_5Me_5)_2Ln$ units in polymetallic organolanthanide complexes. The preferred tetrahedral disposition of C_5Me_5 ring centroids in **2**, which clearly has a variety of available geometries, reemphasizes the preference for this arrangement already found in $[(C_5Me_5)_2Sm]_2(\mu\text{-}O)$,[55] $[(C_5Me_5)_2Sm(\mu\text{-}H)]_2$, and $(C_5Me_5)_2ClY(\mu\text{-}Cl)Y(C_5Me_5)_2$. If a $(C_5Me_5)_2Ln$ unit cannot satisfy its coordination needs *and* have a tetrahedral ring centroid arrangement in a bimetallic complex, it will adopt a more highly oligomerized form which has a greater distance between $(C_5Me_5)_2Ln$ units. Hence unsolvated $(C_5Me_5)_2SmCl$ trimerizes. Given the importance of bridging vs. nonbridging ligands to reactivity,[2] knowledge of the tendency of a system to oligomerize is essential to understanding reactivity patterns.

Finally, the structural data on **1** and **2** emphasize further the remarkable nature of $[(C_5Me_5)_2Sm(\mu\text{-}H)]_2$. The small size of the hydride ligands allows this $(C_5Me_5)_2SmZ$ system to achieve eight coordination in a dimeric structure with a tetrahedral arrangement of the C_5Me_5 rings. This may not be possible with ligands other than hydride.

Acknowledgment. We thank the National Science Foundation for support of the research, the Alfred P. Sloan Foundation for a Research Fellowship (to W.J.E.), and Simon Bott for help with the crystallography.

Supplementary Material Available: Completely numbered plot of the cation in **2** and tables of bond distances, angles, and thermal parameters (7 pages); tables of observed and calculated structure factors (40 pages). Ordering information is given on any current masthead page.

(53) Li, X.-F.; Fischer, R. D. 1st International Conference on Chemistry and Technology of Lanthanides and Actinides; Venice, Italy, September, 1983, A22, *Inorg. Chim. Acta* **1983**, *94*, 51-52.
(54) Li, X.-F.; Feng, X.-Z.; Xu, Y.-T.; Wang, H.-T.; Shi, J.; Liu, L.; Sun, P.-N. *Inorg. Chim. Acta* **1986**, *116*, 85-93.
(55) Evans, W. J.; Grate, J. W.; Bloom, I.; Hunter, W. E.; Atwood, J. L. *J. Am. Chem. Soc.* **1985**, *107*, 405-409.

Formation of Imidates, Amides, Amines, Carbamates, and Ureas from the μ_3-NPh Ligands of $Fe_3(\mu_3\text{-}NPh)_2(CO)_9$

Gregory D. Williams,[†] R. R. Whittle,[†] Gregory L. Geoffroy,*[†] and Arnold L. Rheingold[‡]

Contribution from the Departments of Chemistry, The Pennsylvania State University, University Park, Pennsylvania 16802, and University of Delaware, Newark, Delaware 19711.
Received October 29, 1986

Abstract: The bis(nitrene) cluster $Fe_3(\mu_3\text{-}NPh)_2(CO)_9$ (**1**) reacts with $Li[HBEt_3]$, MeLi, PhLi, and NaOMe to form the formyl and acyl clusters $[Fe_3(\mu_3\text{-}NPh)_2(CO)_8C\{O\}R]^-$ (**4**, R = H; **6**, R = Ph; **7**, R = Me; **8**, R = OMe). Formyl cluster **4** is unstable at room temperature and slowly loses CO to form the hydride cluster $[HFe_3(\mu_3\text{-}NPh)_2(CO)_8]^-$. The benzoyl cluster **7** reacts with EtOTf to yield the nitrene-carbene cluster $Fe_3(\mu_3\text{-}NPh)_2(CO)_8(C\{OEt\}Ph)$ (**9**) which has been structurally characterized: *Pbca*, a = 13.668 (6) Å, b = 17.588 (7) Å, c = 25.644 (8) Å, V = 6164 (7) Å^3, Z = 8, R = 0.060, R_w = 0.075 for 2982 reflections with $F_o > 2\sigma(F_o)$. The carbene ligand is bound to a basal iron atom, and the carbene carbon lies within the Fe_3 plane. The carbene and nitrene ligands in **9** couple to form the imidate PhN=C(OEt)Ph when **9** is exposed to air or allowed to stand in solution for prolonged periods under CO or N_2 atmospheres. A crossover experiment showed this coupling to be strictly intramolecular. Similar nitrene-benzoyl coupling from **7** gives benzanilide, and the methoxycarbonyl and nitrene ligands in **8** couple to give methyl *N*-phenylcarbamate when the clusters are oxidatively degraded with $[FeCp_2]^+$. The latter reaction models mechanistic suggestions previously made for the $M_3(CO)_{12}$ (M = Fe, Ru) catalyzed carbonylation of $PhNO_2$ to yield carbamates. The bis(phosphinidene) cluster $Fe_3(\mu_3\text{-}PPh)_2(CO)_9$ (**2**) also reacts with PhLi to yield a benzoyl derivative, $[Fe_3(\mu_3\text{-}PPh)_2(CO)_8(C\{O\}Ph)]^-$. However, addition of EtOTf to this species does not result in a carbene cluster analogous to **9**, but instead phosphinidene-carbene coupling occurs to give $Fe_3(\mu_3\text{-}PPh)(\mu_3\text{-}PhPC\{OEt\}Ph)(CO)_9$ which has been structurally characterized: $P\bar{1}$, a = 9.241 (2) Å, b = 10.233 (3) Å, c = 19.564 (5) Å, α = 84.53 (2)°, β = 84.43 (2)°, γ = 76.41 (2)°, V = 1784.7 (8) Å^3, Z = 2, R = 0.0557, R_w = 0.0602 for 3710 reflections with $F_o > 3\sigma(F_o)$. The phosphorus atom of the μ_3-PhPC{OEt}Ph ligand bridges two iron atoms, and the ethoxy-substituted carbon is attached to the third iron atom.

The chemistry of low-valent metal carbene complexes has been extensively investigated, and many such compounds have found impressive synthetic utility.[1] In contrast, the chemistry of *nitrene* ligands bound to low-valent metals remains relatively unexplored,[2] even though such ligands have been invoked as intermediates in several catalytic reactions.[3] The lack of chemical studies is in part due to the low stability of *mononuclear* carbonyl nitrene complexes such as $(CO)_5Cr{=}NPh$,[4] a particularly interesting species in view of the large number of synthetic applications of its carbene analogue.[1c] Like many reactive organic ligands, stabilization of nitrenes by low-valent organometallics can be

[†] The Pennsylvania State University.
[‡] University of Delaware.

(1) (a) Brown, F. J. *Prog. Inorg. Chem.* **1980**, *27*, 1. (b) Casey, C. P. *React. Intermed.* **1985**, *3*, 109. (c) Kreissl, F. R.; Doetz, K. H.; Weiss, K. In *Transition Metal Carbene Complexes*; Verlag Chemie: Weinheim, 1983. (d) Collman, J. P.; Hegedus, L. S. *Principals and Applications of Organotransition Metal Chemistry*, University Science Books: Mill Valley, CA, 1980; pp 91-103.
(2) For reviews, see: (a) Nugent, W. A.; Haymore, B. L. *Coord. Chem. Rev.* **1980**, *31*, 123-175. (b) Cenini, S.; La Monica, G. *Inorg. Chim. Acta* **1976**, *18*, 279.

0002-7863/87/1509-3936$01.50/0

Scheme I

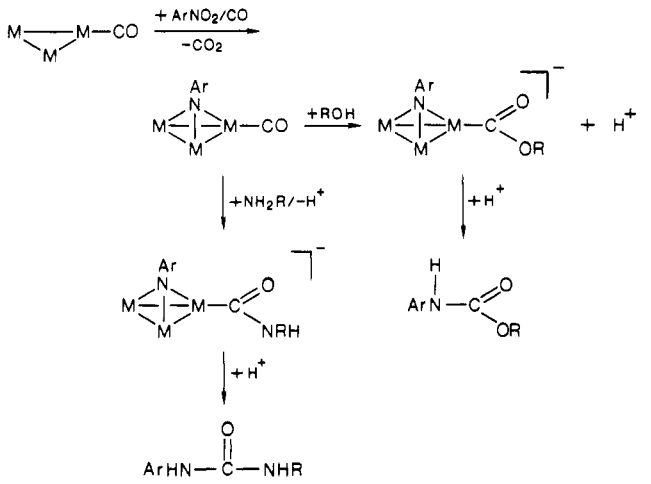

achieved through coordination of the ligand to adjacent metals in cluster compounds, with the μ_3-NR coordination mode being most common.[1] Although several such μ_3-nitrene clusters are known,[3e-h,5] relatively little is understood about their chemical properties.[1,3e-g,5a,j,o]

A particularly important example of a catalytic reaction that has been suggested to proceed via nitrenes is the carbonylation of nitroaromatics to produce isocyanates, carbamates (urethanes), and ureas.[3a-d] Nitroaromatics are relatively inexpensive, and their use avoids the intermediacy of phosgene and toxic isocyanates for the industrial production of ureas and carbamates which find usage as important insecticides.[6] Both homogeneous and heterogeneous catalysts are known for these carbonylations, with the former typically giving greater selectivities for the desired products.[3a-c,7]

Scheme II

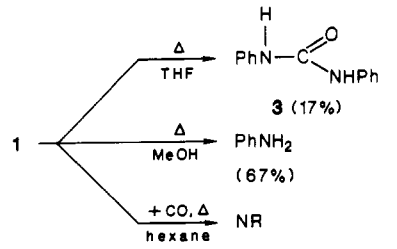

The mechanisms of these reactions are unknown, but two specific examples for which the intermediacy of nitrene containing clusters has been invoked are shown in eq 1 and 2.[3a,b] The former reaction

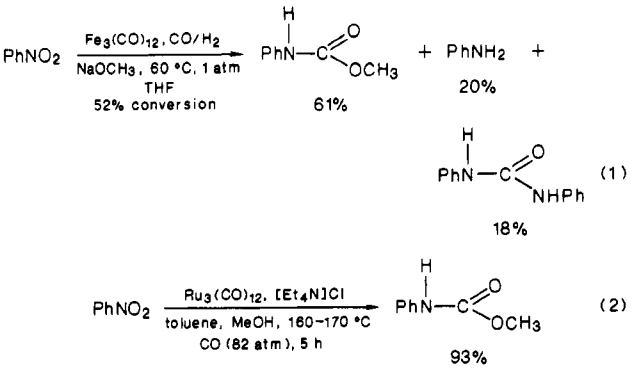

gives a mixture of products whereas the latter halide promoted system gives good selectivity to methyl *N*-phenylcarbamate. It is known that both $Fe_3(CO)_{12}$ and $Ru_3(CO)_{12}$ react with $PhNO_2$ to yield CO_2 and the nitrene-containing clusters of types I and II,[5a,d,e] and in both of the above catalytic processes the intermediacy of a cluster such as III, formed via methoxide addition to a carbonyl ligand, was suggested.[3a,b] Coupling of the methoxy-

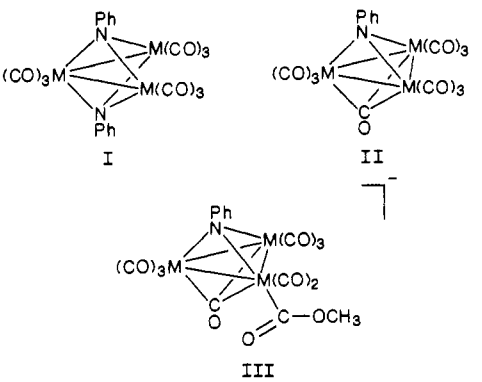

carbonyl and nitrene ligands in III followed by protonation would give the observed carbamate product (Scheme I). Ureas could form via a similar process (Scheme I) involving reduction of some fraction of $PhNO_2$ to aniline,[3d,g] followed by the formation of a carbamoyl ligand analogous to the methoxycarbonyl ligand in III.

The goals of the research described herein were twofold. We first wished to develop the fundamental chemistry of coordinated μ_3-nitrene ligands and accordingly examined the reactions of $Fe_3(\mu_3\text{-}NPh)_2(CO)_9$ (**1**),[5d] a representative compound, with CO, HBR_3^-, RLi, NaOMe, and $ArNH_2$ reagents. As described herein these have led to nitrene clusters which also possess formyl, hydride, acyl, carbene, and methoxycarbonyl ligands. In the course of this research we undertook a comparative study of similar chemistry with the analogous phosphinidene cluster $Fe_3(\mu_3\text{-}PPh)_2(CO)_9$ (**2**),[8] and those results are also described. The second goal of this research was to test the validity of the mechanisms suggested in Scheme I by preparing and examining clusters similar to III. This research has shown that the nitrene ligands in these

(3) (a) Cenini, S.; Pizzotti, M.; Crotti, C.; Porta, F.; La Monica, G. *J. Chem. Soc., Chem. Commun.*, **1984**, 1286. (b) Alper, H.; Hashem, K. E. *J. Am. Chem. Soc.* **1981**, *103*, 6514. (c) des Abbayes, H.; Alper, H. *J. Am. Chem. Soc.* **1977**, *99*, 98. (d) L'Eplattenier, F.; Matthys, P.; Calderazzo, F. *Inorg. Chem.* **1970**, *9*, 342. (e) Andrews, M. A.; Kaesz, H. D. *J. Am. Chem. Soc.* **1979**, *101*, 7255. (f) Dawoodi, Z.; Mays, M. J.; Henrick, K. *J. Chem. Soc., Dalton Trans.* **1984**, 433. (g) Bhaduri, S.; Gopalkrishnan, K. S.; Clegg, W.; Jones, P. G.; Sheldrick, G. M.; Stalke, D. *J. Chem. Soc., Dalton Trans.* **1984**, 1765.

(4) Hegedus, L. S.; Kramer, A. *Organometallics* **1984**, *3*, 1263.

(5) (a) Sappa, E.; Milone, L. *J. Organomet. Chem.* **1973**, *61*, 383. (b) Koerner von Gustorf, E.; Wagner, R. *Angew. Chem., Int. Ed. Engl.* **1971**, *10*, 910. (c) Barnett, B. L.; Kruger, C. *Angew. Chem., Int. Ed. Engl.* **1971**, *10*, 910. (d) Stanghellini, P. L.; Rossetti, R. *Atti Accad. Sci. Torino*, **1970**, *105*, 391. (e) Aime, S.; Gervasio, G.; Milone, L.; Rossetti, R.; Stanghellini, P. L. *J. Chem. Soc., Dalton Trans.* **1978**, 534. (f) Doedens, R. J. *Inorg. Chem.* **1969**, *8*, 570. (g) Otsuka, S.; Nakamura, A.; Yoshida, T. *Inorg. Chem.* **1968**, *7*, 261. (h) Yin, C. C.; Deeming, A. J. *J. Chem. Soc., Dalton Trans.* **1974**, 1013. (i) Lin, Y. C.; Knobler, C. B.; Kaesz, H. D. *J. Am. Chem. Soc.* **1981**, *103*, 1216. (j) Lin, Y. C.; Knobler, C. B.; Kaesz, H. D. *J. Organomet. Chem.* **1981**, *213*, C41. (k) Bhaduri, S.; Gopalkrishnan, K. S.; Sheldrick, G. A.; Clegg, W.; Stalke, D. *J. Chem. Soc., Dalton Trans.* **1983**, 2339. (l) Smieja, J. A.; Gladfelter, W. L. *Inorg. Chem.* **1986**, *25*, 2667. (m) Smieja, J. A.; Gozum, J. E.; Gladfelter, W. L. *Organometallics* **1986**, *5*, 2154. (n) Blohm, M. L.; Gladfelter, W. L. *Organometallics* **1986**, *5*, 1049. (o) Bernhardt, W.; Von Schnering, C.; Vahrenkamp, H. *Angew. Chem., Int. Ed. Engl.* **1986**, *25*, 279. (p) Bernhardt, W.; Vahrenkamp, H. *Angew. Chem., Int. Ed. Engl.* **1984**, *23*, 381. Bagga, M. M.; Flannigan, W. T.; Knox, G. R.; Pauson, P. L.; Preston, F. J.; Reed, R. I. *Chem. Commun.* **1968**, 36. (q) Flannigan, W. T.; Knox, G. R.; Pauson, P. L. *Chem. Ind. (London)* **1967**, 1094. (r) Dekker, M.; Knox, G. R. *Chem. Commun.* **1967**, 1243.

(6) Hartley, G. S.; West, T. F. *Chemicals for Pest Control*; Pergamon: New York, 1969; pp 86-89, 174-183.

(7) (a) Alessio, E.; Mestroni, G. *J. Organomet. Chem.* **1985**, *291*, 117. (b) Dieck, H. A.; Laine, R. M.; Heck, R. F. *J. Org. Chem.* **1975**, *40*, 2819. (c) Yamashita, M.; Mizushima, K.; Watanabe, Y.; Mitsudo, T.; Takegami, Y. *J. Chem. Soc., Chem. Commun.* **1976**, 670. (d) Nefedov, B. K.; Manov-Yuvenskii, V. I. *Izv. Akad. Nauk SSSR, Ser. Khim.* **1977**, *11*, 2597. (e) Nefedov, B. K.; Manov-Yuvenskii, V. I.; Khoshdurdyev, *Dokl. Akad. Nauk SSSR* **1977**, *232*, 1088. (f) Elleuch, B.; Taarit, Y. B.; Basset, J. M.; Kervennal, J. *Angew. Chem., Int. Ed. Engl.* **1982**, *21*, 687. (g) Weigert, F. J. *J. Org. Chem.* **1973**, *38*, 1316. (h) Hardy, W. B.; Bennett, R. P. *Tetrahedron Lett.* **1967**, 961. (i) Unverferth, K.; Hontsch, R.; Schwetlick, K. *J. Prakt. Chem.* **1978**, *321*, 928. (j) Braunstein, P.; Bender, R.; Kervennal, J. *Organometallics* **1982**, *1*, 1236 and references therein. (k) Braunstein, P.; Kervennal, J.; Richert, J.-L. *Angew. Chem., Int. Ed. Engl.* **1985**, *24*, 768.

(8) Bartsch, R.; Hietkamp, S.; Morton, S.; Stelzer, O. *J. Organomet. Chem.* **1981**, *222*, 263.

clusters are reactive and can be induced to couple with several of the above ligands to produce imidates, amides, carbamates, and ureas.[9]

Results

Formation of Diphenylurea and Aniline upon Thermal Decomposition of $Fe_3(\mu_3\text{-NPh})_2(CO)_9$ (1). Cluster **1** slowly decomposes over a period of weeks at 22 °C or within 5–6 h at 65 °C in degassed or N_2-saturated THF solutions to form a tan insoluble residue and diphenylurea (**3**) in low yield (Scheme II). The added hydrogens in **3** likely come from solvent abstraction, adventitious water, or the chromatographic workup. The yield of **3** increased to 25% upon the addition of 2 equiv of aniline to the refluxing solutions of **1** while addition of *p*-toluidine gave **3** (7%), tolylphenylurea (17%), and ditolylurea (1%). A control experiment in which *p*-toluidine and **3** were combined in refluxing THF for 12 h in the absence of iron-containing organometallics showed that **3** did not convert into tolylphenylurea under these conditions. When a mixture of **1** and **1**-d_{10} were refluxed in THF, the isolated diphenylurea consisted of 35% **3**-d_0, 37% **3**-d_5, and 29% **3**-d_{10}, indicating that the formation of **3** from **1** occurs largely by an intermolecular path.

Aniline was produced in 72% yield when the decomposition of **1** was conducted in refluxing methanol under N_2 (Scheme II). This reaction presumably proceeds by sequential protonation of the nitrene ligands of **1** by methanol. It also may be relevant to the mechanism of the rapid catalytic production of aromatic amines from nitroaromatics using a $Fe_3(CO)_{12}$/MeOH mixture.[10] A trace of azobenzene was formed in this reaction, but no diphenylurea nor methyl *N*-phenylcarbamate (see below) were detected.

Attempted Reaction of 1 with CO. Many clusters fragment to lower nuclearity products when heated in the presence of CO. Such reaction of **1** with CO could also yield isocyanates from carbonylation of the μ_3-NPh ligands. However, **1** is particularly resistant to carbonylation and was recovered in ~80% yield after heating under 1000 psi CO pressure at 80 °C for 12 h (Scheme II) with no new ν_{CO} bands detected in the IR spectrum of the reaction solution. This result suggests that the instability of **1** in the absence of CO as outlined above is likely due to a decomposition process that is initiated by CO dissociation. Other work has shown that the CO ligands of **1** rapidly exchange with added CO.[11]

Reaction of 1 with $Li[HBEt_3]$ To Form the Formyl Cluster $Li[Fe_3(\mu_3\text{-NPh})_2(CO)_8(C\{O\}H)]$ (4). Formyl cluster **4** results when $Li[HBEt_3]$ is added to **1** (eq 3). Cluster **4** was not sufficiently

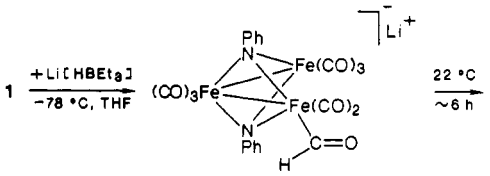

4

$$Li[HFe_3(\mu_3\text{-NPh})_2(CO)_8] \quad (3)$$

5

stable to isolate, but it was spectroscopically characterized. The presence of the formyl ligand was indicated by the 1595 cm^{-1} ν_{CO} band and a downfield ^1H NMR resonance at δ 14.52. The formyl ligand is assumed to be on the Fe atom indicated in the drawing in eq 3 by analogy to the site of acyl and carbene formation described below. Following the terminology used by others,[12] the

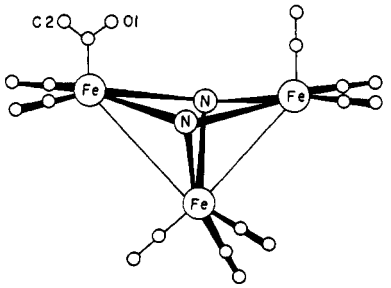

Figure 1. A drawing of **9** that illustrates the square-pyramidal geometry of the cluster core. The upper two Fe atoms and the nitrogens form the basal plane of the square-pyramid, and these Fe atoms are labeled as the basal irons. The bottom Fe atom is termed axial.

unique Fe atom in **1** which is bonded to two other Fe atoms is designated as the axial Fe, and the two equivalent Fe atoms are termed basal Fe atoms. These designations refer to the approximately square-pyramidal geometry of the cluster as depicted in Figure 1 for the carbene cluster **9** (see below).

Formyl cluster **4** is stable in solution at −78 °C, but at 22 °C it undergoes CO loss and deinsertion with a $t_{1/2}$ of ca. 1.5 h to give the hydride cluster **5** (eq 3). This species was isolated as a dark red oil that slowly decomposed over 1–2 days in N_2-saturated solutions. It showed a hydride ^1H NMR resonance at δ −20.48 which suggests a structure with a bridging hydride.[13] In addition to bands in the terminal ν_{CO} region, its IR spectrum showed two bands at 1827 and 1795 cm^{-1} that imply the presence of μ-CO ligands. The rate of the deinsertion reaction was unaffected by addition of 9,10-dihydroanthracene, arguing against a radical chain mechanism for the formyl to hydride conversion.[14]

Protonation and methylation of the formyl cluster $[Os_3(CO)_{11}(CHO)]^-$ convert the formyl ligand into a μ-methylene ligand in $Os_3(CO)_{11}(\mu\text{-}CH_2)$.[15] However, formyl cluster **4** gave only regeneration of **1** upon treatment with $CH_3OSO_2CF_3$ or H_3PO_4, presumably via evolution of CH_4 and H_2, respectively. Similar reactions have been reported for mononuclear anionic formyl complexes.[16]

Formation of the Acyl Clusters $[Fe_3(\mu_3\text{-NPh})_2(CO)_8(C\{O\}R)]^-$ (R = Ph, Me, OMe) from Reaction of 1 with RLi and NaOMe. Acyl-substituted clusters **6–8** form upon reaction of **1** with MeLi, PhLi, and NaOMe (eq 4). Each of these can be isolated as red

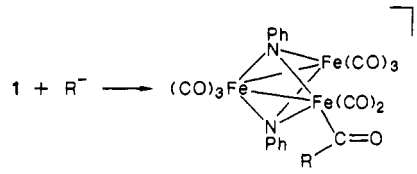

(4)

6, R = Ph (94%)
7, R = Me (85%)
8, R = OMe

solids, although they were typically prepared and used in situ. They each show similar terminal ν_{CO} bands as well as IR bands assigned to the acyl ligands (**6**, 1543 cm^{-1}; **7**, 1592 cm^{-1}; **8**, 1620 cm^{-1}). Complex **6** has a characteristic acyl ^{13}C NMR resonance at δ 264.3 and has been further characterized by its conversion to the structurally characterized carbene substituted cluster **9** (see below). The latter shows the carbene ligand to be bound to a basal Fe, and the acyl ligand is presumably bound to the same Fe atom, as indicated in eq 4. Similar structures are assumed for **7** and **8**.

(9) A preliminary account of part of this work has been published: Williams, G. D.; Geoffroy, G. L.; Whittle, R. R.; Rheingold, A. L. *J. Am. Chem. Soc.* **1985**, *107*, 729.

(10) Landesburg, J. M.; Katz, L.; Olsen, C. *J. Org. Chem.* **1972**, *37*, 930.

(11) Rossetti, R.; Stanghellini, P. L. *J. Coord. Chem.* **1974**, *3*, 217.

(12) (a) Aime, S.; Milone, L.; Rossetti, R.; Stanghellini, P. L. *J. Chem. Soc., Dalton Trans.* **1980**, 46. (b) Cook, S. L.; Evans, J.; Gray, L. R. *J. Organomet. Chem.* **1982**, *236*, 367. (c) Kouba, J. K.; Muetterties, E. L.; Thompson, M. R.; Day, V. W. *Organometallics* **1983**, *2*, 1065.

(13) (a) Deeming, A. J.; Hasso, S. *J. Organomet. Chem.* **1976**, *114*, 313. (b) Smieja, J. A.; Gladfelter, W. L. *J. Organomet. Chem.* **1985**, *297*, 349.

(14) (a) Sumner, C. E.; Nelson, G. O. *J. Am. Chem. Soc.* **1984**, *106*, 432. (b) Barratt, D. S.; Cole-Hamilton, D. J. *J. Chem. Soc., Chem. Commun.* **1985**, 458. (c) Paonessa, R. S.; Thomas, N. C.; Halpern, J. *J. Am. Chem. Soc.* **1985**, *107*, 4333. (d) Narayanan, B. A.; Amatore, C.; Kochi, J. K. *Organometallics* **1986**, *5*, 926.

(15) Steinmetz, G. R.; Morrison, E. D.; Geoffroy, G. L. *J. Am. Chem. Soc.* **1984**, *106*, 2559.

(16) Gladysz, J. A. *Adv. Organomet. Chem.* **1982**, *20*, 1.

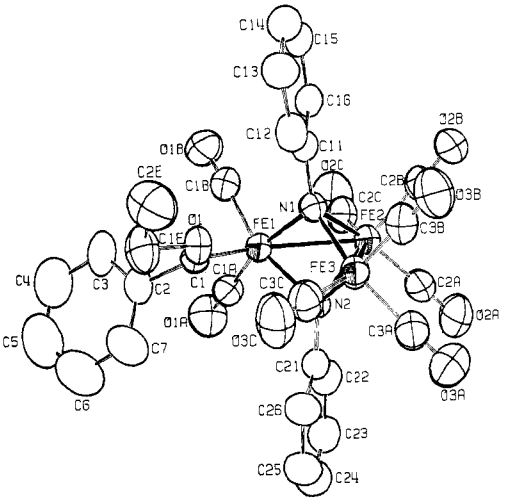

Figure 2. An ORTEP drawing of $Fe_3(\mu_3\text{-NPh})_2(CO)_8\{C\{OEt\}Ph\}$ (**9**). Thermal ellipsoids are drawn at the 40% probability level.

The ^{13}C NMR spectrum of **8** shows no resonance which can be assigned to the methoxycarbonyl ligand, apparently because of rapid exchange of methoxide between the carbonyls and free methoxide ion, similar to that found for $[Ru_3(CO)_{11}(CO_2Me)]^-$.[17] The metal carbonyl ^{13}C NMR resonance of **8** is a singlet at δ 223.2, shifted 15.4 ppm downfield from the weighted average of the carbonyl resonances of **1**. A similar singlet shifted 7.3 ppm downfield was observed upon forming $[Ru_3(CO)_{11}(CO_2Me)]^-$ from $Ru_3(CO)_{12}$.[17a] This was attributed to an averaging of the positions of the metal carbonyl and methoxycarbonyl resonances due to rapid exchange of the methoxide between carbonyls. Such an exchange process also presumably occurs with **8**. Addition of acids to methanol solutions of **8** quantitatively re-formed **1**, and exchange of CD_3O^- for CH_3O^- occurred when **8** was isolated and then redissolved in CD_3OD. Likewise, dissolution of **8** in THF and Et_2O gave slow reversal of reaction 4 and re-formation of **1**.

Synthesis of the Nitrene–Carbene Cluster $Fe_3(\mu_3\text{-NPh})_2(CO)_8(C\{OEt\}Ph)$ (9). The nitrene–carbene cluster **9** readily formed upon addition of EtOTf to **6** (eq 5). This species was

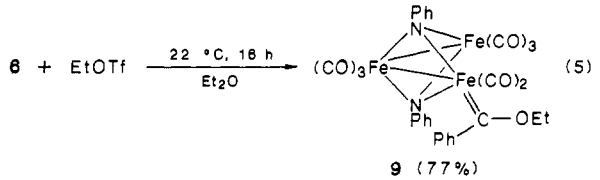

(5)

isolated as a red crystalline solid and characterized by X-ray diffraction (Figure 2). Its ^1H NMR spectrum shows the expected resonances for the ethoxy substituent, and its ^{13}C NMR spectrum displays a singlet at δ 326.8 attributed to the carbene carbon. At −40 °C the ^{13}C NMR spectrum also shows a carbonyl resonance at δ 214.2 (3 CO) assigned to three averaged carbonyls on the axial iron atom, a resonance at δ 213.4 (1 CO) attributed to the single unique carbonyl on the basal Fe atom not possessing the carbene ligand, and two resonances at δ 207.6 (2 CO) and 203.2 (2 CO) due to the two pairs of equivalent carbonyls on the basal Fe atoms. These assignments are similar to those made for other $Fe_3(\mu_3\text{-X})_2(CO)_8L$ clusters.[12a,c] The δ 207.6 resonance broadens as the sample is warmed to room temperature, but little change occurs in the remaining resonances. However, the thermal instability of the compound described below has prevented a detailed analysis of this broadening process. Protonation, rather than alkylation, of the benzoyl cluster **6** resulted in the regeneration of **1** and formation of benzaldehyde, possibly via an unstable hydroxy–carbene intermediate.[18]

Table I. Crystallographic Data for $Fe_3(\mu_3\text{-NPh})_2(CO)_8(C\{OEt\}Ph)$ (**9**) and $Fe_3(\mu_3\text{-PPh})(\mu_3\text{-PhPC}\{OEt\}Ph)(CO)_9$ (**16**)

	9	**16**
	(a) Crystal Parameters	
mol wt	708.03	770.0[a]
crystal system	orthorhombic	triclinic
space group	*Pbca*	$P\bar{1}$
a, Å	13.668 (6)	9.241 (2)
b, Å	17.588 (7)	10.233 (3)
c, Å	25.644 (8)	19.564 (5)
α, deg	90	84.53 (2)
β, deg	90	84.43 (2)
γ, deg	90	76.41 (2)
V, Å^3	6164 (7)	1784.7 (8)
Z	8	2
μ, cm^{-1}	14.45	13.7
ρ, g cm^{-3} (calcd)	1.526	1.43[a]
size, mm	0.26 × 0.90 × 1.25	0.21 × 0.24 × 0.29
	(b) Data Collection	
diffractometer	Enraf-Nonius CAD4	Nicolet R3
radiation	Mo Kα (λ = 0.71073 Å)	Mo Kα (λ = 0.71073 Å)
monochromator	graphite	graphite
2θ scan range, deg	3.2–45.6	4–45
scan type	θ–2θ	ω
scan spd, deg min^{-1}	1–5	var 5–20
temp, °C	21	23
std rflns	3 h^{-1}	3 std/197 rflns
	(c) Data Reduction and Refinement	
rflns collected	4638	4991
unique rflns	3520	4643
unique rflns with $F_o \geq n\sigma(F_o)$	2982 (n = 2)	3710 (n = 3)
R_F,[b] %	6.0	5.57
R_{wF}, % (g = 0.001)[b]	7.5	6.02
highest peak, final diff Fourier, e Å^{-3}	0.74	1.21[c]

[a] Does not include contributions from severely distorted hexane molecule(s) of uncertain stoichiometry. [b] $w^{-1} = \sigma^2(F_o) + g(F_o^2)$; $R_F = \sum|\Delta|/\sum|F_o|$; $R_{wF} = \sum(|\Delta|w^{1/2})/\sum(|F_o|w^{1/2})$; $\Delta = |F_o| - |F_c|$. [c] Top five peaks associated with disordered hexane molecule(s) followed by diffuse background (<0.4 e Å^{-3}).

X-ray Diffraction Study of $Fe_3(\mu_3\text{-NPh})_2(CO)_8(C\{OEt\}Ph)$ (9). An ORTEP drawing of **9** is shown in Figure 2, and the important structural parameters are given in Tables I–III. The structure is similar to that established for **1**[19] except that the carbene ligand has replaced a basal carbonyl ligand. It consists of an open triangle of Fe atoms with the capping μ_3-NPh ligands lying above and below the Fe_3 triangle. The Fe–Fe bond lengths, the Fe(1)–Fe(2)–Fe(3) angle, and the Fe–N distances are all similar to those found in **1**.[19]

The three iron atoms and the carbene carbon C(1) are nearly coplanar with C(1) lying only 0.166 Å above the Fe_3 plane. The dihedral angle between the Fe_3 plane and the carbene carbon and its substituents ([Fe(1)–Fe(2)–Fe(3)]–[O(1)–C(1)–C(2)]) is 33.6°. Few Fe–carbene complexes have been crystallographically characterized, but the iron–carbene Fe(1)–C(1) distance of 1.856 (5) Å is similar to the 1.819 (3) Å distance found in $(CO)_3FeC(OCH_3)C(CO_2CH_3)=C(H)CO_2CH_3$.[20]

Formation of the Imidate PhN=C(OEt)Ph (10) via Nitrene–Carbene Coupling from 9. Although cluster **9** is stable as a crystalline solid, solutions under N_2 or vacuum at 22 °C slowly decompose over ~1 week to form the imidate **10** along with tan insoluble organometallic residues (eq 6). Imidate **10** was formed

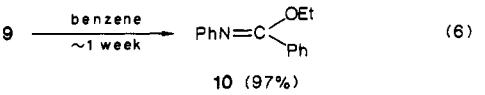

(6)

(17) (a) Darensbourg, D. J.; Gray, R. L.; Pala, M. *Organometallics* **1984**, *3*, 1928. (b) Gross, D. C.; Ford, P. C. *J. Am. Chem. Soc.* **1985**, *107*, 585.
(18) (a) Fischer, E. O.; Maasboe, A. *Angew. Chem., Int. Ed. Engl.* **1964**, *3*, 580. (b) Ryang, M.; Rhee, I.; Tsutsumi, S. *Bull. Chem. Soc. Jpn.* **1964**, *37*, 341. (c) Fischer, E. O. *Adv. Organomet. Chem.* **1976**, *14*, 1.

(19) Clegg, W.; Sheldrick, G. M.; Stalke, D.; Bhaduri, S.; Khwaja, H. K. *Acta Crystallogr., Sect. C: Cryst. Struct. Commun.* **1984**, *C40*, 2045.
(20) Nakatsu, K.; Mitsudo, T.; Nakanishi, H.; Watanabi, Y.; Takegami, Y. *Chem. Lett.* **1977**, 1447.

Table II. Atomic Coordinates and Temperature Factors for $Fe_3(\mu_3\text{-NPh})_2(CO)_8(C\{OEt\}Ph)$ (**9**)

atom	x	y	z	U_{iso},[a] Å^2
Fe(1)	0.28932 (7)	0.11683 (5)	0.15306 (4)	3.22 (2)
Fe(2)	0.11054 (7)	0.13575 (6)	0.16868 (4)	3.56 (2)
Fe(3)	0.16026 (8)	0.25528 (6)	0.13030 (4)	3.97 (2)
O(1)	0.4162 (3)	0.2360 (3)	0.1412 (2)	4.1 (1)
O(1A)	0.3380 (5)	-0.0232 (3)	0.0952 (2)	6.4 (2)
O(1B)	0.3810 (4)	0.0451 (3)	0.2443 (2)	5.9 (1)
O(2A)	-0.0662 (5)	0.0946 (4)	0.1111 (3)	9.3 (2)
O(2B)	-0.0027 (4)	0.2001 (3)	0.2544 (2)	6.0 (1)
O(2C)	0.1367 (5)	-0.0143 (3)	0.2152 (3)	9.1 (2)
O(3A)	-0.0018 (5)	0.2773 (4)	0.0572 (2)	9.6 (2)
O(3B)	0.0764 (5)	0.3765 (3)	0.1946 (2)	7.1 (2)
O(3C)	0.3064 (4)	0.3494 (4)	0.0773 (3)	8.1 (2)
N(1)	0.2235 (4)	0.2009 (3)	0.1870 (2)	3.3 (1)
N(2)	0.1912 (4)	0.1540 (3)	0.1054 (2)	3.6 (1)
C(1)	0.4057 (5)	0.1635 (4)	0.1339 (2)	3.4 (1)
C(1E)	0.5118 (6)	0.2758 (5)	0.1297 (4)	6.1 (2)
C(2E)	0.5142 (9)	0.3476 (6)	0.1619 (4)	8.4 (3)
C(1A)	0.3177 (5)	0.0312 (4)	0.1173 (3)	4.4 (2)
C(1B)	0.3460 (5)	0.0757 (4)	0.2104 (3)	4.1 (2)
C(2A)	0.0046 (6)	0.1094 (5)	0.1341 (3)	5.6 (2)
C(2B)	0.0409 (5)	0.1744 (4)	0.2209 (3)	4.2 (2)
C(2C)	0.1318 (6)	0.0457 (5)	0.1960 (3)	5.3 (2)
C(3A)	0.0626 (7)	0.2703 (5)	0.0841 (3)	5.9 (2)
C(3B)	0.1101 (6)	0.3292 (4)	0.1702 (3)	4.8 (2)
C(3C)	0.2510 (6)	0.3123 (4)	0.0983 (3)	5.3 (2)
C(2)	0.4873 (5)	0.1215 (4)	0.1085 (3)	4.3 (2)
C(3)	0.5461 (6)	0.0717 (5)	0.1367 (4)	6.2 (2)
C(4)	0.6175 (8)	0.0304 (7)	0.1089 (5)	9.2 (3)
C(5)	0.6279 (8)	0.0396 (7)	0.0553 (5)	10.0 (3)
C(6)	0.5665 (9)	0.0865 (7)	0.0280 (4)	10.0 (3)
C(7)	0.4987 (8)	0.1305 (6)	0.0544 (3)	7.7 (2)
C(11)	0.2516 (5)	0.2302 (4)	0.2370 (3)	3.7 (1)
C(12)	0.2924 (5)	0.3033 (4)	0.2400 (3)	4.8 (2)
C(13)	0.3256 (6)	0.3326 (5)	0.2873 (3)	5.7 (2)
C(14)	0.3143 (6)	0.2875 (5)	0.3335 (3)	6.0 (2)
C(15)	0.2720 (6)	0.2159 (5)	0.3307 (3)	5.4 (2)
C(16)	0.2391 (5)	0.1852 (4)	0.2819 (3)	4.4 (2)
C(21)	0.1775 (5)	0.1234 (5)	0.0539 (3)	4.7 (2)
C(22)	0.1390 (6)	0.0497 (5)	0.0457 (3)	5.7 (2)
C(23)	0.1272 (6)	0.0230 (6)	-0.0053 (3)	7.1 (2)
C(24)	0.1517 (7)	0.0687 (6)	-0.0466 (4)	7.6 (3)
C(25)	0.1897 (7)	0.1392 (6)	-0.0399 (4)	7.4 (3)
C(26)	0.2054 (6)	0.1708 (6)	0.0116 (3)	6.5 (2)

[a] Equivalent isotropic U defined as one-third of the trace of the orthogonal U_{ij} tensor.

Table III. Selected Bond Distances and Angles for $Fe_3(\mu_3\text{-NPh})_2(CO)_8(C\{OEt\}Ph)$ (**9**)

	(a) Bond Distances (Å)		
Fe(1)-Fe(2)	2.498 (1)	Fe(3)-N(1)	1.944 (4)
Fe(2)-Fe(3)	2.419 (1)	Fe(1)-N(2)	1.929 (4)
Fe(1)-C(1)	1.856 (5)	Fe(2)-N(2)	1.988 (4)
Fe(1)-N(1)	1.937 (4)	Fe(3)-N(2)	1.939 (4)
Fe(2)-N(1)	1.980 (4)	O(1)-C(1)	1.297 (5)
	(b) Bond Angles (deg)		
Fe(1)-Fe(2)-Fe(3)	77.04 (3)	Fe(2)-N(2)-Fe(3)	76.0 (1)
Fe(1)-N(1)-Fe(2)	79.3 (1)	N(1)-Fe(1)-C(1)	100.3 (2)
Fe(1)-N(1)-Fe(3)	104.2 (2)	Fe(2)-Fe(1)-C(1)	145.2 (2)
Fe(1)-N(2)-Fe(2)	79.2 (2)	N(2)-Fe(1)-C(1)	106.1 (2)
Fe(1)-N(2)-Fe(3)	104.7 (2)	Fe(1)-C(1)-O(1)	119.4 (4)
Fe(2)-N(1)-Fe(3)	76.1 (1)	Fe(1)-C(1)-C(2)	122.6 (4)

in high yield and characterized by comparison of its spectroscopic data to those of an authentic sample.[21] It must derive by coupling of the nitrene and carbene ligands of **9**, as confirmed by the labeling studies discussed below.

Nitrene–carbene coupling also occurs when the reaction is conducted under a CO atmosphere to give imidate **10** and the known cluster $Fe_3(\mu_3\text{-NPh})(CO)_{10}$ (**11**)[3e] (eq 7). This reaction is accelerated at 50 °C and is complete within 12 h. Note that

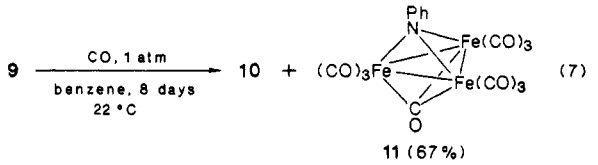

(7)

11 (67%)

cluster **11** is precisely the product expected from displacing the nitrene and carbene ligands by two CO's and the generation of an additional Fe–Fe bond. When a near equimolar mixture of **9**-d_0 and **9**-d_{15} with perdeuteriated phenyl groups was allowed to react with CO, the isolated imidate consisted of 51% **10**-d_0, <0.1% **10**-d_5, and 49% **10**-d_{10}, indicating that the nitrene–carbene coupling proceeds by a strictly *intramolecular* process.

The nitrene–carbene coupling process is accelerated in the presence of air such that the decomposition of **9** in solution is complete within ca. 3 days. The effect of air is apparently to induce cluster decomposition by oxidation (see below). A double-labeling experiment similar to that described above showed that the air-induced nitrene–carbene coupling to form **10** is also intramolecular (see Experimental Section). Ethyl benzoate, formed by oxidation of the carbene ligand,[1a] is also a product of this latter reaction.

Electrochemical Studies of 1 and 9. For a comparison of the behavior of **1** and **9** toward oxidation, cyclic voltammetry was performed on each. Cluster **1** showed an irreversible oxidation wave at +1.08 V at a scan rate of 20 mV/s, but partially reversibility was apparent at a scan rate of 200 mV/s. These results are similar to those reported for $Fe_3(\mu_3\text{-S})_2(CO)_9$[22] (+1.3 V, irreversible) and $Fe_3(\mu_3\text{-PPh})_2(CO)_9$ (**2**) (+1.37 V, irreversible).[23] The carbene cluster **9** shows an irreversible oxidation wave at +0.65 V at scan rates of 20 and 100 mV/s. Note that replacing a CO in **1** with the carbene ligand in **9** makes the cluster easier to oxidize by 0.35 V. The relative ease of oxidation of **9** is reflected in the acceleration of the carbene–nitrene coupling described above by air-induced oxidation.

Formation of Benzanilide via Nitrene–Benzoyl Coupling from 6. Solutions of the benzoyl cluster **6** are stable at 22 °C under N_2 for long periods, but exposure to air results in decomposition within ca. 15 min to give benzanilide along with a tan insoluble precipitate (eq 8). Benzanilide logically derives from coupling

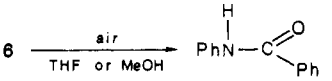

(8)

12 (64%)

of the nitrene and carbene ligands with the added proton likely coming from solvent or adventitious water. The coupling is immediate if the mild oxidizing agent $[Cp_2Fe]^+$ is used to induce the decomposition, and the yield of benzanilide is slightly higher (73%). This reaction is stoichiometric but not catalytic in $[Cp_2Fe]^+$.

Unlike the intramolecular character of the nitrene–carbene couplings discussed above, a double-labeling experiment showed that the nitrene–benzoyl coupling proceeds largely by an *intermolecular* path. When methanol solutions of **6**-d_0 and **6**-d_{15} were exposed to $[Cp_2Fe]^+$, the benzanilide isolated consisted of 31% **12**-d_0, 38% **12**-d_5, and 31% **12**-d_{10}. Oxidation apparently induces cluster degradation since the nitrene and benzoyl ligands from the resulting fragments combine in a nearly random process.

Formation of Methyl *N*-Phenylcarbamate via Nitrene–Methoxycarbonyl Coupling from 8. Methyl *N*-phenylcarbamate (**13**) was produced from nitrene–methoxycarbonyl coupling when the methoxycarbonyl cluster **8** was heated in methanol solution (eq 9). The added proton in **13** likely comes from the methanol

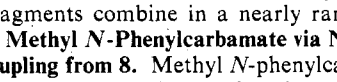

(9)

13 (18%)

(21) Lander, G. D. *J. Chem. Soc.* **1902**, 591.

(22) Madach, T.; Vahrenkamp, H. *Chem. Ber.* **1981**, *114*, 505.

(23) Ohst, H. H.; Kochi, J. K. *J. Am. Chem. Soc.* **1986**, *108*, 2897.

solvent or SiO_2 chromatographic workup. Air or $[Cp_2Fe]^+$-induced oxidation of methanol solutions of **8** also gave **13**, with a significantly higher yield (61%) when $[Cp_2Fe]^+$ was employed.

Methyl *N*-phenylcarbamate was also formed in good yield when cluster **1** was subjected to conditions identical with those used by Alper and co-workers[3b] in the $Fe_3(CO)_{12}$-catalyzed carbonylation of $PhNO_2$ to produce **13** (eq 10). This reaction likely proceeds via the in situ formation of methoxycarbonyl cluster **8**, followed by nitrene–methoxycarbonyl coupling.

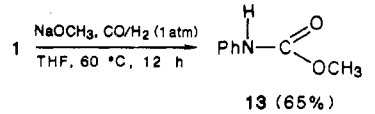

13 (65%) (10)

Formation of $[Fe_3(\mu_3\text{-PPh})(\mu_2\text{-PHPh})(CO)_9]^-$ upon Reaction of 2 with $Li[HBEt_3]$. The phosphinidene cluster $Fe_3(\mu_3\text{-PPh})_2(CO)_9$ (**2**) has previously been shown to react with borohydride reagents to form the phosphido cluster **14** (eq 11).[24] This reaction

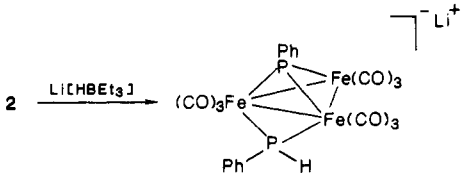

14 (11)

was examined in detail to determine if an unstable formyl cluster similar to **4** forms initially. This could give **14** by CO deinsertion to give a hydride ligand followed by hydride–phosphinidene coupling. Note that Shyu and Wojicki[25] showed that the complex $[Fe_2(\mu\text{-PPh}_2)(CO)_6(PPh_2H)]^-$ forms from $Fe_2(\mu\text{-PPh}_2)_2(CO)_6$ and $[HBEt_3]^-$ via spectroscopically detectable formyl and hydride intermediates. However, IR monitoring of the reaction of **2** with $Li[HBEt_3]$ at −40 °C showed the clean conversion to **14** with no detectable intermediates. Thus, if a formyl cluster is formed, it must rapidly deinsert even at these low temperatures. Alternatively, **14** could form by direct addition of hydride to a phosphinidene ligand.[26]

Formation of the Benzoyl Cluster $[Fe_3(\mu_3\text{-PPh})_2(CO)_8(C\{O\}Ph)]^-$ from Reaction of 2 with PhLi. The phosphinidene cluster **2** reacts cleanly with PhLi to generate the new benzoyl cluster **15** (eq 12).

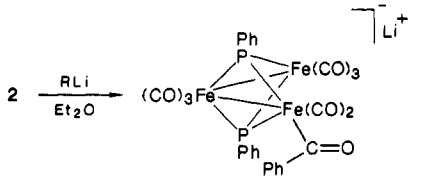

15 (12)

This species has been spectroscopically characterized. Its IR spectrum shows a benzoyl ν_{CO} band at 1535 cm^{-1} and terminal ν_{CO} bands similar to those of the nitrene–benzoyl cluster **6**. A single broad resonance at δ 226.8 in its 22 °C ^{31}P NMR spectrum is assigned to the presumably equivalent μ-PPh ligands. Although reaction 12 proceeded rapidly at −78 and 22 °C, addition of excess PhLi led to rapid decomposition of **15** and use of impure **2** also gave a significantly reduced yield of **15**. This may explain the earlier failure to obtain tractable products from the reaction of **2** with PhLi.[24a]

Phosphinidene–Carbene Coupling To Form $Fe_3(\mu_3\text{-PPh})(\mu_3\text{-PhPC\{OEt\}Ph})(CO)_9$ (16). Benzoyl cluster **15** was treated with EtOTf in an attempt to prepare a phosphinidene–carbene cluster analogous to the nitrene–carbene cluster **9**. However, the isolated

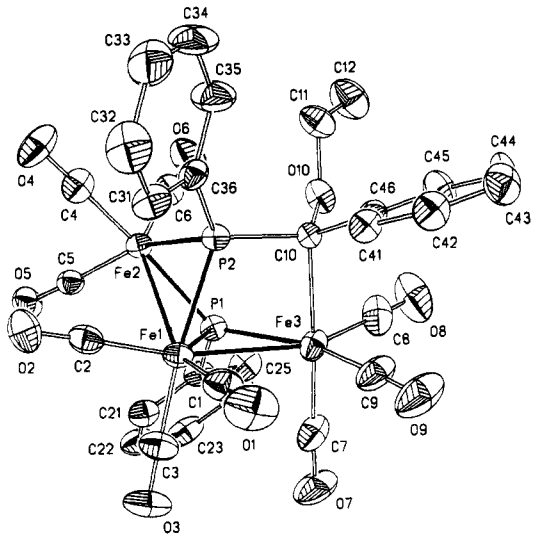

Figure 3. An ORTEP drawing of $Fe_3(\mu_3\text{-PPh})(\mu_3\text{-PhPC\{OEt\}Ph})(CO)_9$ (**16**). Thermal ellipsoids are drawn at the 40% probability level.

product of this reaction was cluster **16** which formed via phosphinidene–carbene coupling (eq 13). The crystal structure of

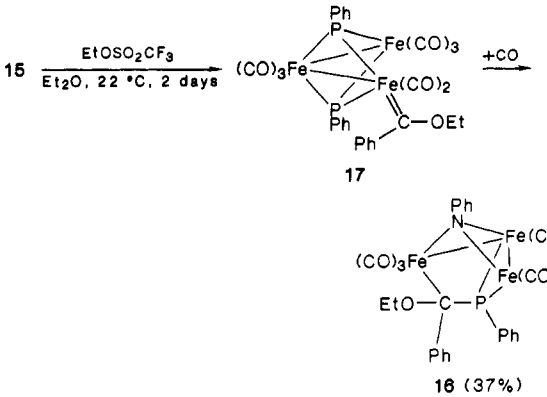

(13)

16, Figure 3, shows the phosphorus atom of the μ_3-PhPC(OEt)Ph ligand to bridge two iron atoms with carbon C(10) bound to the third iron atom. The carbon and phosphorus atoms of this ligand are chiral giving four possible stereoisomers consisting of two diastereomeric pairs. The ^1H and ^{31}P NMR data summarized in the Experimental Section show that the diastereomers are formed in equal abundance, but no attempt was made to separate them.

The formation of **16** proceeds via a detectable but unstable intermediate which is presumably the phosphinidene–carbene cluster **17** (eq 13). If the reaction is stopped after 16 h and chromatographed on SiO_2, **16** is isolated in 17% yield along with a dark red oily compound which shows IR bands at 2056 (m), 2018 (s,br), 2002 (m), 1975 (m,sh), and 1963 (m,br) cm^{-1} similar to those of the nitrene–carbene cluster **9**. Solutions of this species became cloudy over 1–2 h, and chromatography of the resultant solution gave **16** as the only eluting organometallic complex. Although the ^{31}P NMR spectrum of the reaction mixture was complex, ^{13}C NMR monitoring of the reaction showed the growth and then disappearance of a carbene resonance at δ 321.7, similar to that of **9** at δ 326.8.

The formation of the two diastereomers of **16** in equal amounts can be understood by first assuming that the structure of the intermediate phosphinidene–carbene cluster **17** is similar to that of the structurally characterized nitrene–carbene cluster **9**, with the carbene carbon lying within the plane of the Fe_3 triangle. The P–C linkage in **16** can then result from coupling of the carbene carbon with either phosphinidene ligand giving the two diastereomers as long as carbene rotation or other significant cluster reorganization did not occur during the coupling process. The reaction can be viewed as addition of a phosphorus atom to either

(24) (a) O'Connor, J. P. Ph.D. Thesis, University of Wisconsin-Madison, 1977. (b) Ohst, H. H.; Kochi, J. K. *Inorg. Chem.* **1986**, *25*, 2066.
(25) Shyu, S.-G.; Wojcicki, A. *Organometallics* **1985**, *4*, 1457.
(26) Kyba, E. P.; Davis, R. E.; Clubb, C. N.; Liu, S.-T.; Palacios, H. O. A.; McKennis, J. S. *Organometallics* **1986**, *5*, 869.

of the enantiotopic faces of the Fe=C double bond. Since the carbene ligand is presumed to be coplanar with the Fe_3 triangle, there is an equal probability of addition to either Fe=C face, and hence equal amounts of the two diastereomers can form (eq 14).

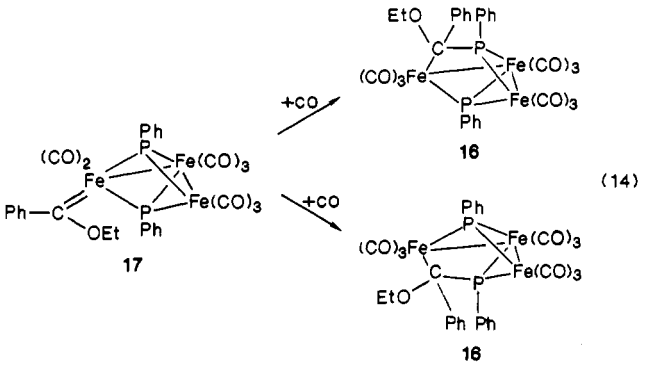

(14)

Molecular Structure of $Fe_3(\mu_3\text{-PPh})(\mu_3\text{-PhPC\{OEt\}Ph})(CO)_9$ (16). An ORTEP drawing of complex **16** is shown in Figure 3, and the important structural parameters are given in Tables I, IV, and V. The molecule has a "butterfly" structure defined by the three iron atoms and P(1) with a PhPC(OEt)Ph ligand bridging the open face of the butterfly. The "hinge" dihedral angle of the butterfly ([Fe(1)–Fe(2)–P(2)]–[Fe(1)–Fe(3)–P(1)]) is 130.1°. Each of the iron atoms is also ligated by three carbonyl ligands. The Fe–Fe distances of 2.671 (2) and 2.750 (1) Å are similar to those reported for its parent **2** (2.718 (3), 2.717 (3), 2.714 (3), 2.717 (3) Å) as are the Fe–P(1) distances (**16**, 2.192 (2)–2.256 (2) Å; **2**, 2.199 (4)–2.231 (5) Å).[12b,27]

The most interesting feature of **16** is the μ_3-PhPC(OEt)Ph ligand. The P(2)—C(10) distance of 1.800 (6) Å is slightly shorter than normal P—C single bond distances of 1.83–1.84 Å[28] but not as short as typical P=C double bond distances of 1.68–1.74 Å.[28] The cluster $Fe_3(CO)_{10}(\mu_3\text{-PhPCH}_2)$ (**18**)[28] has a structure similar to **16**, but the P—C linkage (1.76 (1) Å) of the μ_3-$PhPCH_2$ ligand in **18** was described as having a P=C double bond π-coordinated to the third iron atom. However, a similar description does not

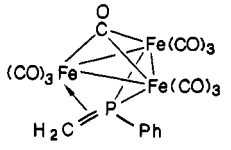

18

appear to be appropriate for **16**. The corresponding P–C distance for **16** is lengthened compared to that in **18** and implies P–C single bond character. Also, the Fe(3)–P(2) distance of 2.947 Å in **16** is far longer than the 2.22-Å average of the other Fe–P distances in **16** and is also longer than typical Fe–P distances in phosphido-bridged iron compounds (e.g., 2.234 (3), 2.228 (3), 2.240 (3), 2.228 (3) Å for $Fe_2(\mu_2\text{-}PPh_2)(CO)_6$[29]), indicating little or no interaction of P(2) with Fe(3). Thus the bonding implied in the drawing of Figure 3 with Fe(3)–C(10) and P(2)–C(10) single bonds appears appropriate.

Discussion

One of the more important aspects of this study is the demonstration that capping nitrene ligands are capable of stabilizing the Fe_3 cluster framework to the point of allowing the preparation of formyl, acyl, and carbene derivatives. This is particularly well-illustrated by the preparation of the formyl cluster **4** which has a stability rivaling that of $[Os_3(CO)_{11}(CHO)]^-$[15] and $[Ir_4(CO)_{11}(CHO)]^-$,[30] the only other cluster formyls known to survive warming to room temperature. The preparation of **4** should be contrasted with the reaction of $Fe_3(CO)_{12}$ with $[BH_4]^-$ which produces only the hydride cluster $[HFe_3(CO)_{11}]^-$.[31] The latter likely forms via rapid deinsertion of an unstable formyl intermediate. Formyl clusters are typically unstable because of the relative ease with which metal–metal bonds can break to open coordination sites for CO deinsertion to occur.[32] This is particularly true for clusters of first- and second-row metals with weak metal–metal bonds, and thus the relative stability of **4** is particularly noteworthy. The stability of the latter can logically be attributed to the rigidity of the cluster framework imposed by the two capping nitrene ligands.

It is also interesting to compare the reaction of **1** with NaOMe to the same reaction with $Fe_3(CO)_{12}$. The latter cluster degrades when treated with NaOMe with no evidence obtained for the formation of a methoxycarbonyl derivative.[17b] In contrast **1** smoothly and quantitatively yields the methoxycarbonyl cluster **8** upon reaction of NaOMe.

A second important conclusion that can be drawn from the results reported herein is that capping nitrene ligands are more inert than are the analogous phosphinidene ligands. Recall that the nitrene cluster **1** cleanly gave the formyl and carbene derivatives **4** and **9** whereas similar reactions with the phosphinidene cluster **2** led to conversion of the phosphinidene ligand into phosphido ligands via phosphinidene–hydride and phosphinidene–carbene coupling. These results indicate that μ_3-PPh ligands will be less useful than μ_3-NPh ligands for imparting cluster stability.

The μ_3-NPh ligands are not inert, however, as evidenced by the novel nitrene–carbene and nitrene–acyl coupling reactions described herein. The detailed mechanisms by which these reactions occur are unknown, although double-labeling experiments clearly showed that the nitrene–carbene coupling to form the imidate **10** occurred by an intramolecular path. The formation of the mononitrene cluster $Fe_3(\mu_3\text{-NPh})(CO)_{10}$ (**11**) from this reaction conducted under a CO atmosphere also argues for intramolecular coupling since this is precisely the product expected upon replacing the nitrene and carbene ligands in **9** with CO. The nitrene–carbene coupling likely proceeds through initial formation of a cluster analogous to the stable product **16** which results from phosphinidene–carbene coupling. The PhP=C(OEt)Ph ligand in **16** is not stable as a free molecule whereas the imidate **10** is, and this may account for the release of the latter from the cluster framework.

As discussed in the Introduction, nitrene–methoxycarbonyl coupling has been proposed as a key step in the $Fe_3(CO)_{12}$ and $Ru_3(CO)_{12}$ catalyzed conversion of nitroaromatics into carbamates (Scheme I),[3a,b] but no direct evidence for such a species was presented. The methoxycarbonyl cluster **8** is an effective model for such an intermediate. As detailed herein **8** does indeed give methyl *N*-phenylcarbamate when thermally or oxidatively degraded, and this reaction represents the first example of the conversion of μ_3-NR ligands into carbamates. These results thus support the suggestion of the intermediacy of nitrene–methoxycarbonyl ligated species in the above-mentioned catalytic reactions. Also relevant to the formation of diphenylurea in the catalytic process (eq 1) is the formation of diarylureas upon thermal decomposition of **1** and upon the reaction of **1** with aniline and *p*-toluidine, supporting the notion that nitrenes may also be precursors to these products (Scheme I). Although clusters have been used in the modeling studies reported here in order to stabilize the nitrene ligands, it is not necessary to invoke the intermediacy of clusters in the catalytic reactions since if nitrenes are involved

(27) There are two crystallographically independent molecules in the unit cell of **2**.[12b]

(28) Knoll, K.; Huttner, G.; Wasiucionek, M.; Zsolnai, L. *Angew. Chem., Int. Ed. Engl.* **1984**, *23*, 739.

(29) Ginsburg, R. E.; Rothrock, R. K.; Finke, R. G.; Collman, J. P.; Dahl, L. F. *J. Am. Chem. Soc.* **1979**, *101*, 6550.

(30) (a) Pruett, R. L.; Schoening, R. C.; Vidal, J. L.; Fiato, R. A. *J. Organomet. Chem.* **1979**, *182*, C57. (b) Schoening, R. C.; Vidal. J. L.; Fiato, R. A. *J. Organomet. Chem.* **1981**, *206*, C43.

(31) Gibson, D. H.; Ahmed, F. U.; Phillips, K. R. *J. Organomet. Chem.* **1981**, *218*, 325.

(32) (a) Rosenberg, S.; Lockledge, S. P.; Geoffroy, G. L. *Organometallics* **1986**, *5*, 2517. (b) Mercer, W. C.; Whittle, R. R.; Burkhardt, E. W.; Geoffroy, G. L. *Organometallics* **1985**, *4*, 68.

they could just as well be formed on dimetal or single metal centers.

Experimental Section

The compounds **1**,[5d] **2**,[8] PhLi-d_5,[33] PhN=C(OEt)Ph,[21,34] and $[Cp_2Fe][PF_6]$[35] were prepared by literature methods or slight modifications thereof. $Fe_3(\mu_3\text{-}NC_6D_5)_2(CO)_9$ (**1**-d_{10}) was prepared by using $C_6D_5NO_2$ in the literature preparation of **1**. Li[$HBEt_3$], PhLi, MeLi, $MeOSO_2CF_3$ (MeOTf), $C_6D_5NO_2$, C_6D_5Br, $PhNH_2$, CF_3CO_2H, ethyl benzoate, and NaOMe (Aldrich Chemical Co.), EtOTf (Alfa Products), CO (CP grade, Matheson or Airco), and ^{13}CO (90% ^{13}C, Monsanto Research Corp.) were purchased and used as received. Solvents used were dried and degassed by standard methods. All manipulations, unless otherwise specified, were conducted under prepurified N_2 by using standard Schlenk and high vacuum line techniques. Instruments used in this research were as previously described.[36] Field desorption (FD) mass spectra were obtained by Dr. Guy Steinmetz and R. J. Hale at the Tennessee Eastman Co., Kingsport, TN. Electron-impact (EI) mass spectra were obtained by using an AEI-MS9 mass spectrometer with a source voltage of 70 eV and probe temperatures in the 50–200 °C range. Gas chromatography was conducted on a 1400 series Varian Aerograph FID gas chromatograph using 10 ft × $^1/_8$ in. Carbopack B or 5 ft × $^1/_8$ in. 1.5% OV-101 on Chrom G columns. Cyclic voltammetry was performed at a glassy carbon electrode using an IBM EC/225 voltammetric analyzer and referenced to SCE. Elemental analyses were performed by Schwartzkopf Microanalytical Laboratory, Woodside, NY.

Thermal Decomposition of 1 in THF Solution. Complex **1** (25 mg, 0.041 mmol) was dissolved in ca. 20 mL of THF and heated to reflux for 16 h. The resultant light orange cloudy solution was cooled and filtered through Celite in air, and the solvent was removed on a rotary evaporator. The tan residue was extracted twice with 1-mL portions of CH_2Cl_2. Chromatography (SiO_2, TLC, Et_2O/hexane, 6:4) gave only a colorless band which contained 1.5 mg of diphenylurea (**3**) (17% yield): IR (KBr) ν_{CO} 1647 cm^{-1}; MS (EI) m/z calcd for $C_{13}H_{12}N_2O$ 212.0950, found 212.0965; ^1H NMR ($CDCl_3$) δ 7.37–7.20 (m, Ph), 6.42 (s, br, N*H*). Thermal decomposition of a mixture of **1**-d_0 and **1**-d_{10} as described above gave **3** whose mass spectrum (EI) showed peaks at m/z 212 (M^+, **3**-d_0), 217 (M^+, **3**-d_5), and 222 (M^+, **3**-d_{10}) in a 35:37:29 ratio.

Thermal Decomposition of 1 in the Presence of Amines. A sample of **1** was thermally decomposed exactly as above except that aniline (7.5 mg, 7.4 μL, 0.082 mmol) was added to the solution. Workup as before gave 2.2 mg of **3** (25% yield). In a similar experiment, **1** (50 mg, 0.082 mmol) was decomposed in THF solution in the presence of 2 equiv of *p*-toluidine. Chromatographic workup gave **3** (1.2 mg, 7% yield), tolylphenylurea (3.2 mg, 17% yield), and ditolylurea (<1% yield), identified by mass spectral analysis (EI).

Thermal Decomposition of 1 in Methanol Solution. Complex **1** (25 mg, 0.041 mmol) was dissolved in 1 mL of methanol, and the solution was heated to reflux for 7 h. The resultant light orange, cloudy solution was cooled and filtered through a pad of Celite in air to remove the brown precipitate which had formed. Gas chromatographic analysis of the light orange solution showed the formation of aniline (5.2 mg, 67% yield). Chromatographic workup (SiO_2, TLC, hexane/CH_2Cl_2, 75:25) yielded a trace of azobenzene (<1 mg), identified by comparison of its IR spectrum to that of an authentic sample.

Attempted Carbonylation of 1. Complex **1** (20 mg, 0.033 mmol) was dissolved in 20 mL of hexane and heated to 80 °C for 12 h under 1000 psi of CO in a high-pressure Parr reactor. The solution was cooled to room temperature and vented. No new ν_{CO} absorbances were observed in the infrared spectrum of the resulting solution, and **1** (16 mg) was recovered in 80% yield.

Reaction of 1 with Li[$HBEt_3$] To Form $[Fe_3(\mu_3\text{-}NPh)_2(CO)_8(CHO)]^-$ (4). A THF solution of Li[$HBEt_3$] (0.083 mL of a 1 M solution) was added dropwise via syringe to a ~20-mL THF solution of **1** (0.050 g, 0.083 mmol) maintained at −78 °C by a dry ice–2-propanol bath. The purple solution turned cherry red upon addition of Li[$HBEt_3$]. At this point the solution showed IR bands at 2050 (m), 2004 (vs), 1997 (s), 1975 (m), 1939 (m), and 1595 (m) cm^{-1} and a ^1H NMR formyl resonance at δ 14.52 (s), indicating the formation of **4**. Upon warmup to 22 °C, the solution darkened and the 1595 cm^{-1} formyl ν_{CO} absorbance decreased in intensity over the course of ca. 5 h as new bands grew in at 2014 (w), 2006 (w), 1966 (s), 1931 (m), 1827 (w), and 1795 (w) cm^{-1}. The δ 14.52 ^1H NMR resonance was replaced by a singlet at δ −20.48 attributed to Li[$HFe_3(\mu_3\text{-}NPh)_2(CO)_8$] (**5**).

Reaction of 4 with MeOTf and H_3PO_4. Solutions of **4**, prepared as described above except with Et_2O as solvent, were treated with MeOTf (0.011 mL, 0.083 mmol) or H_3PO_4 (0.100 mL) at −78 °C and allowed to warm. After the solution was stirred at 0 °C for 1 h, the solvent was removed in vacuo to leave a deep red oil which was chromatographed on silica gel. Elution with hexane/CH_2Cl_2 (8:2) yielded one purple band of **1** (MeOTf reaction, 32 mg, 64% yield; H_3PO_4 reaction, 21 mg, 42% yield).

Preparation of Li[$Fe_3(\mu_3\text{-}NPh)_2(CO)_8(C\{O\}R)$] (R = Ph, Me). A solution of PhLi (2.0 M in cyclohexane/Et_2O, 70:30, 42 μL, 0.083 mmol) or MeLi (1.2 M in Et_2O, 69 μL, 0.083 mmol) was added dropwise via syringe to a THF solution of **1** (50 mg, 0.083 mmol) maintained at −78 °C by a dry ice–2-propanol bath. The purple solution immediately became red and was then allowed to warm to 22 °C. Solvent was removed *in vacuo to yield red microcrystalline* Li[$Fe_3(\mu_3\text{-}NPh)_2(CO)_8(C\{O\}R)$] (**6**, R = Ph, 54 mg, 0.079 mmol, 95%; **7**, R = Me, 44 mg, 0.071 mmol, 85%). These samples persistently gave poor and nonreproducible elemental analyses, apparently due to the retention of variable amounts of solvent. **6**: IR (Et_2O) ν_{CO} 2047 (m), 2006 (vs), 1989 (s), 1973 (s), 1937 (m), 1929 (m), 1586 (m) cm^{-1}; ^{13}C NMR (22 °C, THF-d_8) δ 264.3 (s, *C*OPh), 216.7 (s, 2 *C*O's), 213.6 (s, br, 1 *C*O), 211.4 (s, 2 *C*O's), 210.5 (s, 2 *C*O's), 203.6 (s, br, 1 *C*O). **7**: IR (Et_2O) ν_{CO} 2050 (m), 2006 (s), 1989 (m), 1979 (m), 1946 (m), 1931 (m), 1543 (w) cm^{-1}; ^1H NMR (THF-d_8) δ 2.56 (s, $COCH_3$). These reactions are sensitive to the purity and amount of the added lithium reagent. Use of impure reagents, addition of greater than one equivalent, or fast addition results in substantial decomposition of the resulting acyls.

Reaction of 1 with NaOMe To Give Na[$Fe_3(\mu_3\text{-}NPh)_2(CO)_8(CO_2Me)$] (8). Complex **1** (50 mg, 0.083 mmol) was dissolved in ca. 20 mL of methanol, and NaOMe (6 mg, 0.11 mmol) was added. The color of the solution immediately changed from purple to dark red, and the IR bands of **1** were replaced by new bands at 2046 (w), 2002 (s), 1989 (s), 1964 (m), 1935 (m), and 1620 (w) cm^{-1}. The ^{13}C NMR spectrum (22 °C, CD_3OD) of a similar solution showed a singlet at δ 223.2 (s). Addition of CF_3CO_2H to a solution of **8** gave an immediate red to purple color change and quantitative formation of **1** (by IR).

Preparation of $Fe_3(\mu_3\text{-}NPh)_2(CO)_8(C\{OEt\}Ph)$ (9). A solution of **6**, prepared as described above except in Et_2O solution, was warmed to 22 °C, and EtOTf (0.011 mL, 0.083 mmol) was added via syringe. The solution was stirred for 16 h, and the solvent was removed in vacuo to give a deep red oil which was chromatographed on SiO_2. Elution with hexane/CH_2Cl_2 (85:15) gave a purple band of **1** followed by a deep red band containing 45 mg of **9** (0.063 mmol, 77% yield). Complex **9** was further recrystallized from pentane and isolated as slightly air-sensitive red needles. **9**: IR (hexane) ν_{CO} 2064 (m), 2027 (s), 2017 (m), 2000 (m), 1984 (m), 1959 (m), 1948 (m) cm^{-1}; MS (FD), m/z 708 (M^+); ^1H NMR (22 °C, C_6D_6) δ 6.97–6.33 (m, Ph), 3.98 (q, J = 7.0 Hz, OCH_2CH_3), 0.99 (t, OCH_2CH_3); ^{13}C NMR (−85 °C, CD_2Cl_2) δ 326.8 (s, *C*(OEt)Ph), 214.2 (s, 3 *C*O's), 213.2 (s, 1 *C*O's), 207.6 (s, 2 *C*O's), 203.2 (s, 2 *C*O's).

Formation of PhN=C(OEt)Ph (10) from $Fe_3(\mu_3\text{-}NPh)_2(CO)_8\{C(OEt)Ph\}$ (9). (a) Under Vacuum. Complex **9** (25 mg, 0.035 mmol) was dissolved in ca. 0.5 mL of C_6D_6 and transferred to a 5-mm NMR tube. The solution was degassed by three freeze–pump–thaw cycles and flame sealed under vacuum. Over the course of 8 days the reaction solution became cloudy as the red color faded, and periodic monitoring by ^1H NMR showed that the −OEt resonances due to **9** were replaced by new resonances due to **10** at δ 4.36 (q, J = 7.2 Hz) and 1.20 (t) (97% yield by ^1H NMR integration). The tan organometallic residues were removed from the recovered sample by filtration, and evaporation of solvent gave **10** as a clear oil. **10**: IR (THF) $\nu_{C=N}$ 1657 cm^{-1}; MS (EI), m/z calcd for $C_{15}H_{15}NO$ 225.1154, found 225.1145; ^{13}C NMR (C_6D_6) δ 158.6 (s, *C*=N).

(b) Under CO. Complex **9** (25 mg, 0.035 mmol) was dissolved in ca. 0.5 mL of C_6D_6 and transferred to a 5-mm degassable NMR tube. The solution was degassed by three freeze–pump–thaw cycles, and 1 atm of CO was admitted. No color change occurred over the course of 8 days, although the ethoxy resonances due to **9** were slowly replaced by the resonances due to **10** (95% yield by ^1H NMR integration). In a similar experiment, complex **9** (25 mg, 0.035 mmol) was dissolved in ca. 20 mL of THF and stirred at 22 °C for 8 days under a CO atmosphere. IR monitoring of the reaction showed that absorbances due to **9** were replaced by new bands at 2095 (w), 2053 (s), 2049 (s), 2024 (m), and 1725 (w) cm^{-1} due to $Fe_3(\mu_3\text{-}NPh)(CO)_{10}$ (**11**)[3e] and one at 1657 (w) cm^{-1} due to the imidate **10**. Workup (TLC, SiO_2, hexane/CH_2Cl_2, 85:15) yielded 12 mg of **11** (67% yield, 0.023 mmol, m/z 539 (M^+). When the above reaction was run at 50 °C under flowing CO, IR monitoring showed the

(33) Evans, J. C. W.; Allen, C. F. H. *Organic Syntheses*; Wiley: New York, 1967; Coll. Vol. 2, p 517.
(34) Ta-Shma, R.; Rappoport, Z. *J. Chem. Soc., Perkin Trans. 2* **1977**, 659.
(35) Yang, E. S.; Chan, M.-S.; Wahl, A. C. *J. Phys. Chem.* **1975**, *79*, 2049.
(36) Morrison, E. D.; Geoffroy, G. L. *J. Am. Chem. Soc.* **1985**, *107*, 3541–3545.

complete loss of **9** and formation of **10** and **11** in 12 h.

A similar reaction of an equimolar mixture of **9**-d_0 and **9**-d_{15} at 22 °C for 8 days under a CO atm gave a red oil following evaporation of THF solvent. The red oil was dissolved in a minimum of pentane and cooled to −80 °C. This gave a red crystalline solid from which the mother liquor was separated by decanting. Mass spectral analysis (EI) of the red solid showed it to be an equimolar mixture of **11**-d_0 and **11**-d_5 (m/z 539 and 544 (M^+)). Removal of pentane from the light red mother liquor gave **10** as an oil which showed mass spectral peaks at m/z 225 (M^+, **10**-d_0), 230 (M^+, **10**-d_5), and 235 (M^+, **10**-d_{10}) in a 51:0.005:49 ratio.

(c) In Air. Complex **9** (20 mg, 0.028 mmol) was dissolved in ca. 0.5 mL of C_6D_6 in an NMR tube in air. The red solution turned colorless and cloudy over a 3-day period. After the organometallic residues were filtered off, the solution showed the ^1H NMR resonances of imidate **10** and resonances at δ 4.10 (q, J = 7.2 Hz) and 1.02 (t) due to ethyl benzoate. A similar experiment using **9** that was ^{13}C enriched at both the CO's and the carbene carbon showed two ^{13}C NMR resonances at δ 158.6 and 166.2 due to **10** and ethyl benzoate, respectively. When an approximately equimolar mixture of **9**-d_0 and **9**-d_{15} were exposed to air as described above, a mass spectrum (EI) of the imidate product showed peaks at m/z 225 (**10**-d_0), 230 (**10**-d_5), and 235 (**10**-d_{10}) in a 55:0.004:45 ratio.

Formation of Benzanilide upon Oxidation of $[Fe_3(\mu_3\text{-NPh})_2(CO)_8\{C(O)Ph\}]^-$ (6). Complex **6** (27 mg, 0.039 mmol) was dissolved in ca. 15 mL of methanol and exposed to air or $[Cp_2Fe][PF_6]$ (13 mg, 0.039 mmol) was added. IR monitoring of the reaction showed the disappearance of the ν_{CO} bands of **6** within 15 min after air exposure and less than 5 min after addition of $[Cp_2Fe][PF_6]$. Chromatographic workup (SiO_2, TLC, hexane/CH_2Cl_2, 1:4) gave benzanilide (**12**, 4.9 mg from air exposure, 0.025 mmol, 64% yield; 5.5 mg from $[Cp_2Fe][PF_6]$, 0.028 mmol, 73% yield). **12**: IR (CH_2Cl_2) ν_{CO} 1678 cm^{-1}; MS (EI) m/z calcd for $C_{13}H_{11}NO$ 197.0841, found 197.0835; ^1H NMR (Me_2SO-d_6) δ 10.25 (s, N*H*), 7.96–7.30 (m, Ph). A similar reaction of an equimolar mixture of **6**-d_0 and **6**-d_{15} with $[Cp_2Fe][PF_6]$ gave benzanilide whose mass spectrum showed peaks at m/z 197 (M^+, **12**), 202 (M^+, **12**-d_5), and 207 (M^+, **12**-d_{10}) in a 31:38:31 ratio. A control experiment showed that no crossover occurred between **12**-d_0 and **12**-d_{10} under these reaction conditions.

Formation of Methyl *N*-Phenylcarbamate upon Oxidation of $[Fe_3(\mu_3\text{-NPh})_2(CO)_8\{C(O)OMe\}]^-$ (8). A methanol solution of **8**, generated from **1** (20 mg, 0.033 mmol) and NaOMe (3 mg, 0.05 mmol) as described above, was treated with $[Cp_2Fe][PF_6]$ (11 mg, 0.033 mmol). IR monitoring showed the disappearance of the ν_{CO} bands of **8** within 5 min and chromatographic workup (SiO_2 TLC, hexane/CH_2Cl_2, 1:1) gave 3.0 mg (0.020 mmol, 61% yield) of methyl *N*-phenylcarbamate. **13**: IR (neat film) ν_{CO} 1711 cm^{-1}; MS (EI) m/z calcd for $C_8H_9NO_2$ 151.0633, found 151.0637; ^1H NMR (Me_2SO-d_6) δ 9.63 (s, N*H*), 7.45–6.93 (m, Ph), 3.65 (s, O*CH*$_3$).

Formation of Methyl *N*-Phenylcarbamate upon Thermolysis of 8. A methanol solution of **8**, generated from **1** (50 mg, 0.083 mmol) and NaOMe (7.5 mg, 0.12 mmol) as described above, was heated to 60 °C. The color of the solution lightened, and a tan precipitate formed over the course of 16 h. After the solution was filtered through Celite in air and the solvent was removed by rotary evaporation, workup gave 2.3 mg of methyl *N*-phenylcarbamate (**13**, 18% yield). In a similar experiment, **1** (20 mg, 0.033 mmol) and NaOMe (15 mg, 0.24 mmol) were added to 20 mL of THF. The resulting slurry was transferred to a pressure tube, CO/H_2 (1 atm, 1:1) was admitted, and the mixture was heated to 60 °C for 16 h. Workup of the resultant cloudy solution as above gave 3.1 mg of **13** (0.021 mmol, 65% yield).

Reaction of 2 with Li[HBEt$_3$] To Give $[Fe_3(\mu_3\text{-PPh})(\mu_2\text{-PHPh})(CO)_9]^-$ (14). A THF solution of Li[HBEt$_3$] (79 μL of a 1 M solution) was added dropwise via syringe to a Et_2O solution (ca. 20 mL) of **2** (0.050 g, 0.079 mmol) maintained at −78 °C by a dry ice–2-propanol bath. The orange solution darkened upon addition of Li[HBEt$_3$] and showed IR bands at 2032 (w), 2000 (s), 1962 (s), 1950 (w), and 1890 (w) cm^{-1} which are similar to those reported for **14**.[24a]

Synthesis of the Benzoyl Cluster $[Fe_3(\mu_3\text{-PPh})_2(CO)_8(C\{O\}Ph)]^-$ (15). Phenyllithium (2.0 M in cyclohexane/Et_2O, 70:30, 40 μL, 0.079 mmol) was added dropwise via syringe to a Et_2O solution of **2** (50 mg, 0.079 mmol) which gave an immediate red to dark red color change as **15** formed. This solution showed IR bands at 2050 (m), 2006 (s), 1989 (m), 1979 (m), 1946 (m), 1931 (m), and 1535 (w) cm^{-1}. Solvent evaporation yielded **15** as a red oily solid which showed one broad ^{31}P NMR resonance at δ 226.8 (THF-d_8).

Synthesis of $Fe_3(\mu_3\text{-PPh})(\mu_3\text{-PhPC\{OEt\}Ph})(CO)_9$ (16). EtOTf (15 mg, 11 μL, 0.079 mmol) was added via syringe to a solution of **15**, generated as described above, and the mixture was stirred at room temperature for 2 days. Chromatography (SiO_2, TLC, hexane/CH_2Cl_2, 4:1) gave a rapidly moving red band which contained a small amount of **2** and a second red band of **16** as an equimolar mixture of two diastereomers (24 mg, 0.031 mmol, 37% yield). **16**: IR (Et_2O) ν_{CO} 2072 (w), 2049 (s), 2019 (s), 2008 (m), 1995 (w) cm^{-1}; MS (FD), m/z 770 (M^+); ^1H NMR (C_6D_6) δ 8.06–6.91 (m, Ph), 3.74 (dt, J_{H-H} = 7.2 Hz, J_{H-P} = 7.2 Hz, −OC*H*$_2$CH$_3$), 3.60 (dt, J_{H-H} = 7.2 Hz, J_{H-P} = 7.2 Hz, −OC*H*$_2$CH$_3$), 1.07 (t, br, J_{H-H} = 7.2 Hz, −OCH$_2$C*H*$_3$); $^{31}P\{H\}$ NMR (C_6D_6) δ 301.1 (d, J_{P-P} = 28 Hz), 289.6 (d, J_{P-P} = 23 Hz), 163.7 (J_{P-P} = 28 Hz), 142.7 (J_{P-P} = 23 Hz). Anal. Calcd for $C_{30}H_{20}Fe_3O_{10}P_2$: C, 46.79; H, 2.60. Found: C, 46.68; H, 2.86.

Table IV. Atomic Coordinates (×10^4) and Temperature Factors (Å^2 × 10^3) for $Fe_3(\mu_3\text{-PPh})(\mu_3\text{-PhPC\{OEt\}Ph})(CO)_9$ (**16**)

atom	x	y	z	U_{iso}[a]
Fe(1)	8922 (1)	5434 (1)	1557 (1)	43 (1)
Fe(2)	7176 (1)	3862 (1)	1253 (1)	39 (1)
Fe(3)	6842 (1)	6468 (1)	2586 (1)	52 (1)
P(1)	6407 (2)	5924 (2)	1581 (1)	42 (1)
P(2)	8289 (2)	3712 (2)	2218 (1)	40 (1)
O(1)	11160 (7)	5769 (8)	2439 (4)	108 (3)
O(2)	10920 (6)	3805 (7)	554 (3)	85 (3)
O(3)	8964 (7)	7989 (7)	734 (4)	93 (3)
O(4)	9042 (7)	1193 (6)	937 (3)	90 (3)
O(5)	6752 (6)	4575 (6)	−219 (2)	66 (2)
O(6)	4304 (7)	3171 (7)	1612 (3)	90 (3)
O(7)	6400 (9)	9304 (6)	2040 (4)	108 (3)
O(8)	3960 (8)	6949 (8)	3392 (4)	123 (3)
O(9)	8649 (10)	7046 (7	3632 (4)	122 (4)
O(10)	5618 (5)	4157 (5)	3000 (2)	55 (2)
C(1)	10258 (9)	5631 (9)	2110 (4)	66 (3)
C(2)	10117 (8)	4424 (8)	948 (4)	56 (3)
C(3)	8928 (9)	6988 (9)	1051 (5)	65 (3)
C(4)	8335 (8)	2222 (8)	1064 (4)	61 (3)
C(5)	6891 (7)	4334 (7)	351 (3)	47 (2)
C(6)	5453 (8)	3414 (8)	1476 (4)	56 (3)
C(7)	6572 (10)	8192 (9)	2235 (4)	72 (4)
C(8)	5091 (11)	6766 (9)	3090 (4)	78 (4)
C(9)	7980 (11)	6773 (8)	3225 (4)	79 (4)
C(10)	7110 (6)	4392 (6)	2948 (3)	33 (2)
C(11)	5430 (8)	2832 (9)	3203 (4)	67 (3)
C(12)	3786 (10)	2955 (12)	3414 (5)	99 (5)
C(21)	5569 (5)	7590 (5)	373 (2)	57 (3)
C(22)	4542 (5)	8534 (5)	−4 (2)	74 (4)
C(23)	3115 (5)	9054 (5)	296 (2)	81 (4)
C(24)	2714 (5)	8630 (5)	972 (2)	79 (4)
C(25)	3714 (5)	7687 (5)	1349 (2)	67 (3)
C(26)	5169 (5)	7167 (5)	1049 (2)	49 (3)
C(31)	11169 (5)	2089 (5)	2206 (3)	59 (3)
C(32)	12219 (5)	895 (5)	2351 (3)	93 (5)
C(33)	11766 (5)	−200 (5)	2715 (3)	104 (5)
C(34)	10264 (5)	−99 (5)	2934 (3)	111 (5)
C(35)	9215 (5)	1095 (5)	2788 (3)	86 (4)
C(36)	9667 (5)	2190 (5)	2424 (3)	48 (3)
C(41)	9275 (4)	3806 (5)	3747 (2)	50 (3)
C(42)	9801 (4)	3642 (5)	4402 (2)	65 (3)
C(43)	8794 (4)	3764 (5)	4984 (2)	77 (4)
C(44)	7262 (4)	4051 (5)	4912 (2)	78 (4)
C(45)	6737 (4)	4216 (5)	4257 (2)	68 (3)
C(46)	7743 (4)	4093 (5)	3675 (2)	48 (3)

[a] Equivalent isotropic U defined as one-third of the trace of the orthogonal U_{ij} tensor.

X-ray Diffraction Study of $Fe_3(\mu_3\text{-NPh})_2(CO)_8(C\{OEt\}Ph)$ (9). Red crystals of **9** were grown by slow cooling of a saturated hexane solution of the complex. A suitable crystal was mounted in an arbitrary orientation on a glass fiber on a eucentric goniometer. The Enraf-Nonius programs SEARCH and INDEX were employed to obtain an orientation matrix for data collection and to provide cell dimensions.[37] Details of the data collection and reduction procedures have been previously described.[38] All data were converted to $|F_o|$ values following correction for decay and Lp effects, but an absorption correction was not deemed necessary (μ = 14.45 cm^{-1}). Pertinent crystallographic data are listed in Table I.

The Fe atoms were located by Patterson techniques. The coordinates of the remaining non-hydrogen atoms were determined by successive

(37) Programs used were part of the Enraf-Nonius Structure Determination Package (SDP plus, version 1), Enraf-Nonius, Delft, Holland, 1982.
(38) Horrocks, W. D.; Ishley, J. N.; Whittle, R. R. *Inorg. Chem.* **1982**, *21*, 3265.

Table V. Selected Bond Distances and Angles for $Fe_3(\mu_3\text{-PPh})(\mu_3\text{-PhPC\{OEt\}Ph})(CO)_9$ (16)

(a) Bond Distances (Å)			
Fe(1)-Fe(2)	2.671 (2)	Fe(1)-P(2)	2.240 (2)
Fe(1)-Fe(3)	2.750 (1)	Fe(2)-P(2)	2.211 (2)
Fe(2)-P(1)	2.198 (2)	Fe(3)-C(10)	2.139 (6)
Fe(1)-P(1)	2.256 (2)	P(2)-C(10)	1.800 (6)
Fe(3)-P(1)	2.192 (2)	O(10)-C(10)	1.447 (8)
(b) Bond Angles (deg)			
Fe(2)-Fe(1)-Fe(3)	90.3	Fe(2)-P(1)-Fe(3)	122.3 (1)
Fe(1)-P(2)-Fe(2)	73.7 (1)	Fe(2)-P(2)-C(10)	115.6 (2)
Fe(1)-P(1)-Fe(2)	73.7 (1)	Fe(1)-P(2)-C(10)	107.9 (2)
Fe(1)-P(1)-Fe(3)	76.4 (1)	Fe(3)-C(10)-P(2)	96.5 (3)

least-squares refinements and difference Fourier maps. In the final cycle, least-squares convergence was achieved upon refinement of the positional and anisotropic thermal parameters of all non-hydrogen atoms. A final difference Fourier map showed no unusual peaks; the highest peak of 0.74 e Å^{-3} was located midway between Fe(2) and Fe(3). Final positional parameters are listed in Table II, and relevant bond distances and angles are summarized in Table III.

X-ray Diffraction Study of $Fe_3(\mu_3\text{-PPh})(\mu_3\text{-PhPC\{OEt\}Ph})(CO)_9$ (16). A suitable crystal of **16** was obtained by recrystallization from hexane and was attached to a fine glass fiber with epoxy cement. Unit-cell dimensions were derived from the least-squares fit of the angular settings of 25 reflections, $20° \leq 2\theta \leq 30°$. A profile fitting procedure was applied to all intensity data to improve the precision of the measurement of weak reflections. Details of data collection, reduction, and refinement are listed in Table I.

No correction for absorption was applied to the intensity data due to the low absorption coefficient and regular crystal shape. The three Fe and two P atoms were located by direct methods (SOLV) with remaining non-hydrogen atoms located from subsequent difference Fourier syntheses. All non-hydrogen atoms were refined anisotropically. Hydrogen atoms were assigned idealized, updated locations (d(C-H) = 0.96 Å; $U = 1.2\ U_{iso}$ for the carbon atom to which it was attached). Phenyl carbons were fixed to fit rigid hexagons (d(C-C) = 1.395 Å). The final difference Fourier synthesis showed a disordered solvent molecule of low occupancy presumed to be hexane (maximum, 1.21 e/Å^3) which was not refined. An inspection of F_o vs. F_c values and trends based upon sin θ, Miller index, or parity group failed to reveal any systematic error in the data. All computer programs used in the collection and refinement of crystal data are contained in the Nicolet program packages P3, SHELXTL (version 5.1), and XFG. Atomic coordinates for **16** for the non-hydrogen atoms are provided in Table IV, and selected bond distances and angles are given in Table V.

Acknowledgment. We thank the Department of Energy, Office of Basic Energy Sciences, for supporting this research and the National Science Foundation for contributing funds toward the purchase of the X-ray diffractometer at the University of Delaware. G. Steinmetz and R. J. Hale of the Tennessee Eastman Co. are acknowledged for recording FD mass spectra.

Registry No. 1, 33519-79-8; **1**-d_{10}, 108034-84-0; **3**, 102-07-8; **3**-d_5, 108009-44-5; **3**-d_{10}, 108009-46-7; **4**, 94404-80-5; **5**, 94404-81-6; **6**, 94404-83-8; **6**-d_{15}, 108009-45-6; **7**, 94404-82-7; **8**, 108009-41-2; **9**, 94404-84-9; **9**-d_{15}, 108034-82-8; **10**, 6780-41-2; **10**-d_5, 108034-87-3; **10**-d_{10}, 108034-86-2; **11**, 108034-83-9; **11**-d_5, 108034-85-1; **12**, 93-98-1; **12**-d_5, 108034-88-4; **12**-d_{10}, 108009-47-8; **13**, 2603-10-3; **14**, 108009-42-3; **15**, 94404-85-0; **16** (isomer 1), 108009-43-4; **16** (isomer 2), 108101-11-7; $Li[HBEt_3]$, 22560-16-3; EtOTS, 383-63-1; $[Cp2Fe][PF_6]$, 11077-24-0; *p*-tolylphenylurea, 4300-33-8; ethyl benzoate, 93-89-0.

Supplementary Material Available: Tables of atomic positional and thermal parameters and complete bond lengths and angles for **9** and **16** (8 pages); listings of structure factors for **9** and **16** (36 pages). Ordering information is given on any current masthead page.

Kinetic and Thermodynamic Acidity of Hydrido Transition-Metal Complexes. 4. Kinetic Acidities toward Aniline and Their Use in Identifying Proton-Transfer Mechanisms

Robin T. Edidin, Jeffrey M. Sullivan, and Jack R. Norton*

Contribution from the Department of Chemistry, Colorado State University, Fort Collins, Colorado 80523. *Received April 18, 1986*

Abstract: The kinetic deuterium isotope effects for $CpM(CO)_3H/CpM(CO)_3^-$ (M = Cr, Mo, W) self-exchange reactions in acetonitrile are consistent with a proton-transfer mechanism. The small counterion effect on the rate of self-exchange between $H_2Fe(CO)_4$ and $HFe(CO)_4^-$ is consistent with the absence of IR-observable contact ion pair formation by $[HFe(CO)_4]^-$. Brønsted plots (log of the rate constant vs. log of the equilibrium constant) are linear for proton transfers in acetonitrile from transition-metal hydrides to a series of para-substituted anilines. For $CpW(CO)_3H$ the Brønsted slope, α, is 0.65; for $HMn(CO)_5$ it is 0.54, for $H_2Fe(CO)_4$ it is 0.55, and for $HCo(CO)_4$ it is 0.48. The rates of proton transfer to aniline cover a range of 9 orders of magnitude for the transition-metal hydrides studied: from 1.0×10^{-3} M^{-1} s^{-1} for $HRe(CO)_5$ to 1.7×10^6 M^{-1} s^{-1} for $HCo(CO)_4$. These rates define a kinetic acidity series which for the most part parallels the thermodynamic acidities of these hydrides. This kinetic acidity series has been used to demonstrate that the reaction of $Cp_2Zr(CH_3)_2$ with $CpM(CO)_3H$ (M = Cr, Mo, W) occurs by a proton-transfer mechanism.

In 1982 we commented[1a] that "knowledge of proton-transfer rates (involving transition metals) in straightforward cases should help identify less obvious proton-transfer mechanisms." We then reported comparative rates in CH_3CN for proton transfers from $CpW(CO)_3H$ to $[CpW(CO)_3]^-$ and to morpholine and from $Os(CO)_4H_2$ to $[Os(CO)_4H]^-$ and to Et_3N; these results showed that, for a constant thermodynamic driving force, proton transfers to metal bases faced higher kinetic barriers than proton transfers to nitrogen bases. Pearson, Ford, and co-workers[2] have reported

(1) (a) Part 1: Jordan, R. F.; Norton, J. R. *J. Am. Chem. Soc.* **1982**, *104*, 1255. (b) Part 2: Jordan, R. F.; Norton, J. R. *Acs Symp. Ser.* **1982**, *No. 198*, 403. (c) Part 3: Moore, E. J.; Sullivan, J. M.; Norton, J. R. *J. Am. Chem. Soc.* **1986**, *108*, 2257.

(2) (a) Walker, H. W.; Kresge, C. T.; Pearson, R. G.; Ford, P. C. *J. Am. Chem. Soc.* **1979**, *101*, 7428. (b) Pearson, R. G.; Ford, P. C. *Comments Inorg. Chem.* **1982**, *1*, 279. (c) Walker, H. M.; Pearson, R. G.; Ford, P. C. *J. Am. Chem. Soc.* **1983**, *105*, 1179.

0002-7863/87/1509-3945$01.50/0